

An empirical formulation to predict maximum deformation of blast wall under explosion

Do Kyun Kim^{*1,2}, William Chin Kuan Ng^{1a} and Oeju Hwang^{3b}

¹Ocean and Ship Technology Research Group, Department of Civil and Environmental Engineering, Universiti Teknologi PETRONAS, 32610 Seri Iskandar, Perak, Malaysia

²Graduate Institute of Ferrous Technology, POSTECH, 37673 Pohang, Republic of Korea

³McDermott Asia Pacific, 50250 Kuala Lumpur, Malaysia

(Received July 4, 2018, Revised September 2, 2018, Accepted September 8, 2018)

Abstract. This study proposes an empirical formulation to predict the maximum deformation of offshore blast wall structure that is subjected to impact loading caused by hydrocarbon explosion. The blast wall model is assumed to be supported by a simply-supported boundary condition and corrugated panel is modelled. In total, 1,620 cases of LS-DYNA simulations were conducted to predict the maximum deformation of blast wall, and they were then used as input data for the development of the empirical formulation by regression analysis. Stainless steel was employed as materials and the strain rate effect was also taken into account. For the development of empirical formulation, a wide range of parametric studies were conducted by considering the main design parameters for corrugated panel, such as geometric properties (corrugation angle, breadth, height and thickness) and load profiles (peak pressure and time). In the case of the blast profile, idealised triangular shape is assumed. It is expected that the obtained empirical formulation will be useful for structural designers to predict maximum deformation of blast wall installed in offshore topside structures in the early design stage.

Keywords: empirical formulation; offshore blast wall; explosion; deformation; structural design

1. Introduction

The price of oil, which has fallen dramatically since 2015, has begun to rise gradually to 70 USD per barrel. US Energy Information Administration (EIA)'s Short-Term Energy Outlook (STEO) predicted that Brent crude oil prices will average 71 USD per barrel in 2018, as shown in Fig. 1 (STEO 2018). Due to this, it is reported that shale oil production in the US will also rise by a record-breaking 144,000 bpd from May to June 2018 (OILPRICE 2018). Thus, it is expected that new orders for offshore oil and gas production platforms will also be secured if current oil prices are maintained.

In the case of offshore oil and gas production platforms, an optimization of the topside space is required for the utilization of the installed facilities related to refinement, separation and for the preparation of transportation purposes. Onshore platforms may utilize additional spaces on the land, but due to limited topside area in offshore platforms, the optimization of the topside area is very important. Besides, the health, safety and environment (HSE) issues should also be taken into account in the topside area, which is occupied by hazardous processing

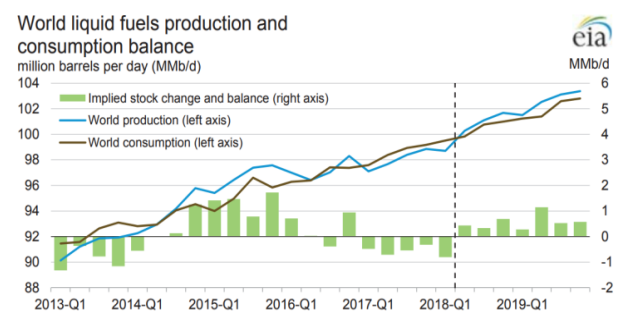


Fig. 1 World liquid fuels production and consumption balance (STEO 2018)

facilities.

In general, it is recommended to install offshore blast wall on the topside of offshore platform, where such a location has a higher possibility of gas leak, to minimise losses and casualties in the event of an explosion (Sohn *et al.* 2014). Meanwhile, information about the potential maximum deformation of blast wall should also be recognised as an important factor to secure the safe path of human inspection on foot. In this regard, a simplified technique for the prediction of maximum deformation of blast wall is required during the early design stage.

Offshore blast walls are basically thin-walled steel structures that are built as an integral part to the topsides of offshore platforms. They serve as a critical safety component to mitigate the consequences of accidental gas explosions in areas where there is risk, e.g., the well bay areas. To protect personnel and critical equipment as well as

*Corresponding author, Senior Lecturer and Adjunct Professor

E-mail: do.kim@utp.edu.my or dokim@postech.ac.kr

^aM.Sc. Student

^bPrincipal Engineer

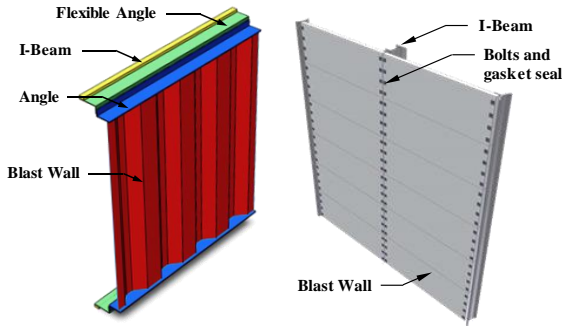


Fig. 2 Corrugated (left) and sandwich (right) blast walls

to prevent the escalation of possible subsequent fires, which may lead to the progressive collapse and loss of integrity of the topsides structure, the design of offshore blast walls commonly includes considerations for large deformations to provide sufficient energy absorption capacities to overcome extreme blast loading (Kim *et al.* 2018b).

Blast walls are normally designed by specialized subcontractors in the form of profiled sheeting, i.e., corrugated panels of steel alloys, and welded onto the primary framework of the topsides. But there are also other designs, for example, in the form of stiffened panels (Pan and Louca 1999, Park and Choi 2006, Sohn *et al.* 2016) and composite panels (Louca and Fallah 2010), as shown in Fig. 2. Recently, a study on other type of blast walls was conducted by Liao and Ma (2018).

Previously, the pioneering work on designs of corrugated panels was performed for ship bulkheads through extensive theoretical and experimental studies. The functions of corrugated bulkheads are to resist axial compressive loads to prevent buckling and to resist lateral loading from hydrostatic pressure in the case of flooding (Caldwell 1955). Paik *et al.* (1997) presented a simple analytical method-based formulation to estimate the ultimate strength of corrugated bulkheads through collapse tests on nine (9) mild steel corrugated bulkhead models that have five (5) bays of corrugations with varying corrugation angle, plate thickness and type of loading, i.e., axial compression and lateral pressure. Liang *et al.* (2006), on the other hand, presented a simplified approximate method for the static plastic analysis of corrugated steel panels by focusing on the relationship between the central panel deformation and the applied distributed load.

In general, the design of blast walls is carried out using 1) single-degree-of-freedom (SDOF) method or 2) an advanced numerical technique known as nonlinear finite element method (NLFEM). Louca *et al.* (2004) summarized the advantages and limitations of the analytical single-degree-of-freedom (SDOF) or the Biggs' method (Biggs 1964) and the numerical nonlinear finite element method (NLFEM) for structural blast analyses. The performance of both methods was also compared and highlighted by Sohn *et al.* (2013) based on the pressure-impulse (P-I) diagrams.

Despite the technological advancements in FEA, the quality of outputs from these numerical analyses strongly depends on the skill and experience of the user. Appropriate modelling techniques, e.g., mesh densities, load and

boundary conditions, material models, and element formulations, are essential to ensure that the FE model represents the real/actual structure. In structural dynamics, much has to be considered for the finite element (FE) formulations governing the parameters of interest for a particular engineering problem.

Boh *et al.* (2004) recommend using the first-order reduced integration shell elements for efficient and accurate FE simulations of blast response. Schwer *et al.* (2005) conducted a three-dimensional (3D) patch test based on the solid mesh proposed by Macneal and Harder (1985) to assess the performance of hourglass control functions via explicit finite element software, LS-DYNA. Sun (2006) demonstrated the compromise between reduced and full integration schemes for FE formulations in dealing with shear locking and hourglassing problems, whereby the details of both problems are as explained by Koh and Kikuchi (1987). As element formulations are intrinsically defined in commercial finite element software, their selection poses a challenge that can directly influence the quality of the solution outputs.

As mentioned above, techniques such as P-I diagram, SDOF method and FE simulations may help structural designers to assess the structural safety of a blast wall structure. There is, however, still demand for a simplified technique or simplified empirical formulation to design the structures efficiently.

In this regard, a simplified empirical formulation that can allow designers to directly predict the maximum deflection of blast wall is investigated in this study by adopting 1,620 cases of parametric study results.

2. Parametric study

In the first step, reliable scenarios need to be selected in order to conduct a parametric study using LS-DYNA and NLFEM. Once the scenarios are confirmed, FE modelling and verification are conducted. The outcome of this parametric study can be used as input data for the development of an empirical formulation.

2.1 Selection of scenarios of blast wall

The structural response of a corrugated blast wall is governed by its geometric configurations, material properties and applied loading conditions as represented in Eq. (1). In this parametric study, all FE models were constructed based on different combinations of geometric parameters, including angle of corrugation (θ), flange breadth (B), web height (H), and panel thickness (t), as illustrated in Fig. 3.

$$w_m = f \left[\underbrace{(\theta, B, H, t, L)}_{\text{Geometry}}, \underbrace{(\sigma_y, E)}_{\text{Material}}, \underbrace{(P_{peak}, t_d)}_{\text{Loading}}, \text{etc.} \right] \quad (1)$$

Geometry Material Loading

The profiles of the corrugated blast wall are symmetrical about the centroidal axis at $H/2$, i.e., having tension and compression flanges of the same dimensions, and the vertical span (or the length of corrugation) of the blast wall

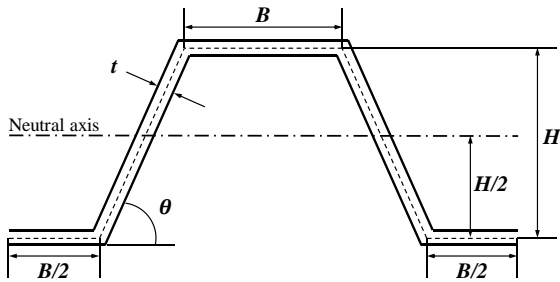


Fig. 3 Cross-sectional parameters of symmetrical corrugation profile for a single corrugation strip

Table 1 Design parameters for corrugated blast walls

Corrugation angle (θ , °)	Breadth (B , mm)	Height (H , mm)	Thickness (t , mm)	Peak pressure (P_{peak} , bar)
50	100	100	6	1
60	120	120	8	3
70	140	140	10	5
80	160	160	-	-
90	180	180	-	-
-	200	200	-	-

Total number of scenarios: $5 \times 6 \times 6 \times 3 \times 3 = 1,620$ cases

Note: 100-milliseconds of duration time (t_d) was adopted based on triangular shape blast profile shown in Fig. 4

models is set to four (4) meters to represent the structures in real scale. Table 1 lists the ranges of the parameters considered in the present study.

In this study, the effects of geometric properties and loading profiles on maximum deformation of corrugated blast wall are investigated, while the effects of material properties are fixed by steel as a single material. In the case of geometric properties, corrugation angle is assumed to be not smaller than 45degree (°) to meet economic efficiency. In this regard, $45 \leq \theta \leq 90$ of corrugation angle range is assumed to be generating the scenarios suggested by Lei *et al.* (2015). In addition, they also suggested the range of the breadth (B), height (H), and thickness (t).

Previously, similar design parameters for the abovementioned corrugated blast walls have been studied by Lei *et al.* (2015). They conducted cost-benefit analysis of corrugated blast walls by assuming 540 cases of scenarios. The difference between the previous and present study is the consideration of the various peak pressure values.

2.2 Finite element modelling

The finite element modelling techniques from Kim *et al.* (2018b) has been adopted in present study. As presented in Fig. 4, a quarter of corrugation strip has been employed to in the FE model, which has been previously verified by experimental data. Fixed boundary condition has been applied to the upper edge of the model, which is assumed to be rigidly connected to the main supporting steelworks of the topsides; on the side and lower edges of the quarter model, symmetrical boundary conditions have been applied.

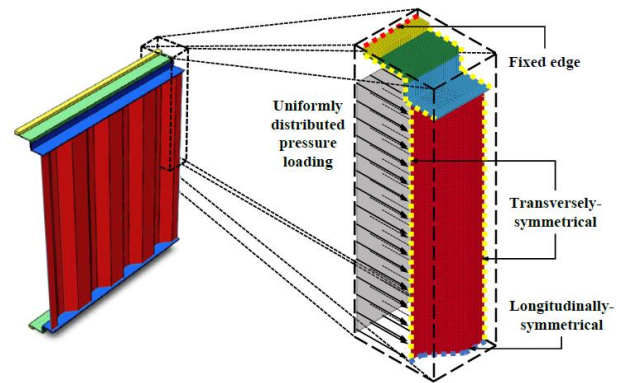


Fig. 4 Quarter section of FE model with load and boundary conditions

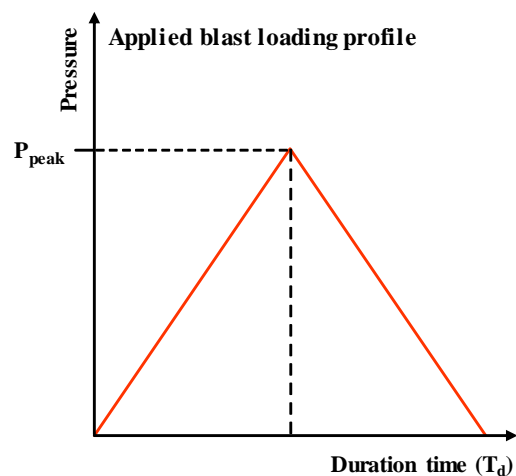


Fig. 5 Idealized triangular blast profile (Lei *et al.* 2015)

The blast pressure is uniformly distributed over the whole of the corrugated panel in the normal directions.

A constant duration time, t_d , of 100-milliseconds was used for all the triangular blast profiles as shown in Fig. 5, which is a typical loading scenario obtainable from computational fluid dynamics (CFD) simulations (Lei *et al.* 2015). As mentioned earlier, in this study, 1,620 cases of scenarios are generated to be analysed by LS-Dyna FE simulation code.

In the case of finite element (FE) types and formulations, Kim *et al.* (2018a) have conducted a wide range of parametric studies. The influence of solid and shell FE formulations with additional hourglass control functions on the maximum response of corrugated blast wall was investigated by using the LS-DYNA explicit FE solver.

In brief, they assumed five (5) cases of finite element type for supporting members (SM) and corrugated panel (CP) by a combination of shell, thick-shell and solid elements as shown in Table A.1(a). They mentioned that Cases 1 and 2 can be used for blast wall analyses with decent accuracies.

- Case 1: SM (Thin-Shell) + CP (Thin-Shell)
- Case 2: SM (Solid) + CP (Thin-Shell)
- Case 3: SM (Solid) + CP (Solid)
- Case 4: SM (Thick-Shell) + CP (Thin-Shell)
- Case 5: SM (Thick-Shell) + CP (Thick-Shell)

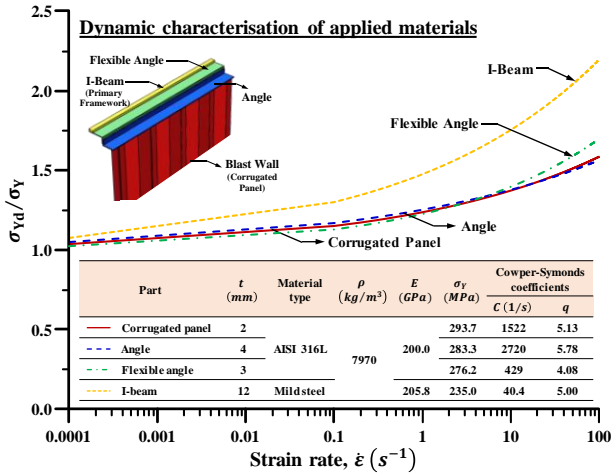


Fig. 6 Dynamic yield strength normalized with static yield strength versus strain rate (Schleyer and Langdon 2003)

Table 2 Structural response domains for different modes of loading (Cormie *et al.* 2009)

Structural response domain	Ratios	
Impulsive	$td/T < 0.1$	$3 < tr/td$
Dynamic	$0.1 < td/T < 10$	$0.3 < tr/td < 3$
Quasi-static	$10 < td/T$	$tr/td < 0.3$

In the case of finite element formulations, they generated four (4) types based on Case 2, as shown in Table A.1(b), and concluded that the use of reduced integration (RI) elements with appropriate hourglass control functions is indeed a cost-effective approach.

- Type I: SM (RI) + CP (RI) + Hourglass control
- Type II: SM (RI) + CP (FI) + Hourglass control
- Type III: SM (FI) + CP (RI) + Hourglass control
- Type IV: SM (FI) + CP (FI)

Note: RI = reduced integration, and FI = full integration.

Based on the outcome of the parametric studies by Kim *et al.* (2018b), a corrugated panel was modelled by shell element with reduced integration and hourglass control (IHQ 5). Details of the parametric study results may be referred to Kim *et al.* (2018b).

In the case of material properties of blast wall, Schleyer and Langdon (2003) conducted a wide range of experimental studies. The summary of material properties of blast wall is shown in Fig. 6, which was also adopted in the parametric study by Kim *et al.* (2018b).

2.3 Characterisation of structural response

Theoretically, structural resonance occurs as the period of the applied blast loading approaches the natural period of the blast wall system. In a vibrating structure, it is important that the design natural periods of the system do not coincide with the periods of the external applied loading to minimize the intensity of possible structural damage due to resonance. However, the concept of “resonance” is not practical in the context of blast analyses as blast waves are not oscillatory in nature.

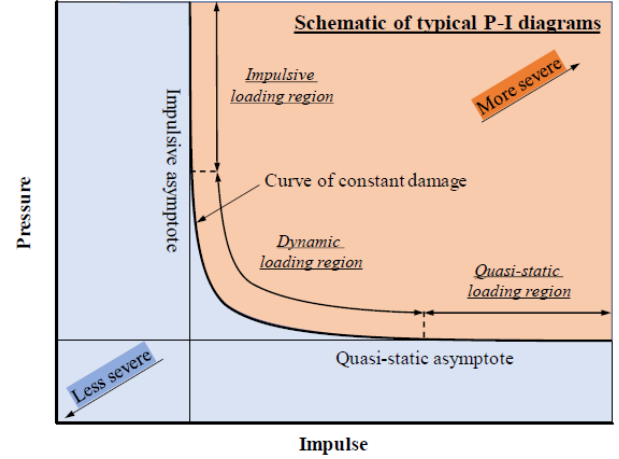


Fig. 7 Pressure-impulse (P-I) iso-damage diagram demonstrating the impulsive, quasi-static, and dynamic response domains

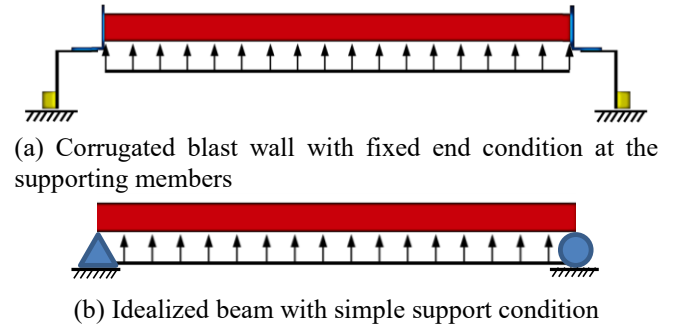


Fig. 8 Assumed blast wall modelling

To assess the blast response of a blast-loaded system, the duration time of the blast load, t_d is obtained with respect to the natural period of the blast-loaded system, i.e., all FE models with different geometric configurations in Table 1. The natural period, T of the structure can be calculated from Eq. (2), and the structural response domains are classified as impulsive, quasi-static, and dynamic subjected to three (3) different modes of blast loading, as summarised in Table 2.

$$T = 2\pi/\omega \quad (2)$$

where $\omega = \sqrt{k/M}$ is the circular frequency of the system, as a function of linear stiffness k and structural mass M . For simply supported beam, $k = 384EI/5L^3$; for clamped beam, $k = 384EI/L^3$ (DNV 2010).

The structural response domains can be illustrated in a pressure-impulse (P-I) or iso-damage diagram, as shown in Fig. 7. It is worth noting that all FE models of different geometric configurations shown in Table 1 fell in the dynamic response domain.

3. Development of empirical formulation

A number of studies have been conducted to provide the closed-form empirical formulations or simplified methods in predicting the accurate results in a short time. In ships

and offshore industry, a wide range of the empirical formulations and simplified techniques have been proposed in terms of prediction of the ultimate strength of hull girder (Caldwell 1965, Paik and Mansour 1995, Paik *et al.* 2012, 2013, Kim *et al.* 2014), stiffened panel (Lin 1985, Paik and Thayamballi 1997, Zhang and Khan 2009, Kim *et al.* 2017, Kim and Lim 2018), unstiffened panel (Smith *et al.* 1988, Ueda *et al.* 1992, Cui and Mansour 1998, Paik *et al.* 2004, Kim *et al.* 2018c), prediction of time-dependent corrosion wastage (Paik and Kim 2012, Mohd Hairil *et al.* 2014), prediction of fatigue and structural performances and other environmental effects (Seo *et al.* 2018, Kim *et al.* 2018a, 2018d).

With regards to blast wall study, in the previous study by Lei *et al.* (2015), a cost-benefit analysis was conducted based on 540 types of corrugated blast walls with design parameters such as corrugation angle (50, 60, 70, 80, 90°), thickness (6, 8, 10 mm), breadth (100, 120, 140, 160, 180, 200 mm), and height (100, 120, 140, 160, 180, 200 mm) under 1 bar of triangular shape loading profile, as shown in Fig. 5.

From their cost-benefit analysis results, they proposed the design criteria by using Pythagorean theorem to calculate the corresponding mass ratio and maximum deflection ratio. In this paper, 3 and 5 bar cases have also been considered. In this study, it may be possible to directly predict the maximum deformation by empirical formulation.

For the development of the empirical formulation used in this study, important parameters were sorted out in advance. The parameters can be summarized based on the geometry of the blast wall (as defined in Fig. 3) and the impulse or loading profile (which is a function of pressure and time). From the given geometry, additional parameters can be calculated, such as the moment of inertia (I), column slenderness ratio (λ), radius of gyration, etc. The expected outcome will be the maximum deflection of the blast wall.

According to the TN5 (Brewerton 1999), each corrugation strip of the blast wall model can be represented by a two-dimensional beam member subjected to lateral distributed load with partially-restrained end conditions, which provide a certain degree of stiffness and moment resistance toward the translational and rotational motions.

Theoretically, the internal reactions of a structural beam member subjected to pure bending are categorized as normal force, shear force and bending moment. While the normal force is assumed to be constant along the span of a homogeneous member with a uniform cross-section, the shear force and bending moment varies with changes in the longitudinal coordinates. Thus, it is reasonable that the actual force distribution across the depth of the beam be expressed as a parameter of the transverse shear force and the bending moment. Both the transverse shear and the bending moment are dependent on the definition of boundary conditions.

As far as boundary condition is concerned, the supporting members at the lower and upper edges are assumed to be clamped, as shown in Fig. 8(a). Isolating the connecting parts from the present FE model, the corrugated panel can then be assumed to behave as a beam simply

supported at both edges, e.g., pin-roller support condition as shown in Fig. 8(b), for the assessment of maximum structural response.

The plastic moment resistance of the simply-supported member due to external loading, M_p , can then be determined in terms of geometric and load properties, whereas the maximum elastic, or yield moment, M_c , is given as a function of geometric and material properties,

$$M_p = \frac{qL^2}{8} \quad (3)$$

$$M_c = \frac{\sigma_y \times I}{c} \quad (4)$$

where $q=P_{peak}A/L$, A = surface area subjected to blast loading, L =span, I =moment of inertia, and c =distance between the neutral axis and the outermost element of the member subjected to bending.

The ratio of M_p/M_c , also known as the shape factor, acts as an indicator for plastic response by determining if the structural deformation has exceeded the yield limit. The load condition, which is governed by the applied peak pressure, P_{peak} , and the duration time, t_d , is expressed in term of impulse, I_p , or by taking the total area under the pressure-time curve. Once again, the assumed simply-supported boundary condition for the calculation of plastic moment, M_p , is shown in Fig. 8(b). The selected 1,620 cases of scenarios illustrated in Table 1 were computed by the LS-DYNA numerical simulation code. The data points for the maximum midspan displacement (or deformation) normalized with the web height, w_m/H , for each FE model are presented with respect to shape factor, M_p/M_c , in Fig. 9.

In order to propose an empirical formulation, a data processing technique is required to be applied. New techniques such as artificial intelligence, machine learning and deep learning-based techniques have been developed and applied in many fields (Kim *et al.* 2018b). In general, regression analysis is widely used. The selected main parameters were related to geometry, and the material properties with applied loading profiles were tested using regression analysis. From the outcome, which is plotted in Fig. 9, we found several trends between maximum deformation normalized with web height (w_m/H) versus shape factor (M_p/M_c). In order to propose the criteria of maximum deformation, additional parameters should be added in the empirical formulation. From the regression analysis, the best parameters, i.e., M_p/M_c , B and H , were selected for the development of the empirical formulation as shown in Fig. 10(a) and (b).

From the present stimulations, it was found that height (H), which directly affects the moment of inertia of the blast wall, has the highest sensitivity to nonlinear structural behaviour among other parameters. In addition, thickness (t) is more sensitive than angle. Similar trends have been observed by Lei *et al.* (2015). These outcomes have been referred to develop an advanced empirical formulation in this study.

Through transformations of the normalized parameters, a “best-fit” 3D surface plot of the normalized deformation

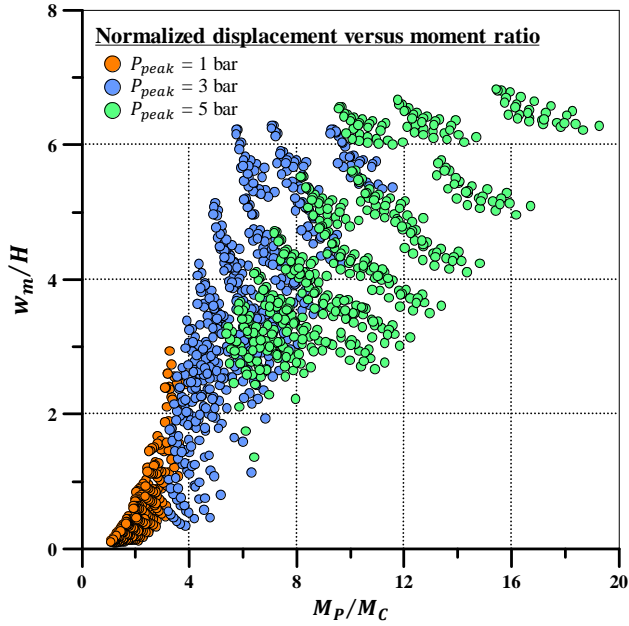


Fig. 9 Normalized deformation, w_m/H versus shape factor, M_P/M_C

with respect to impulse (I_P) and shape factor (M_P/M_C) was generated together with its corresponding 2D plot, as presented in Fig. 10(a) and (b). The surface equation, with an R^2 -value of 0.9212, is given in Eq. (5) which can be considered as the proposed empirical formulation.

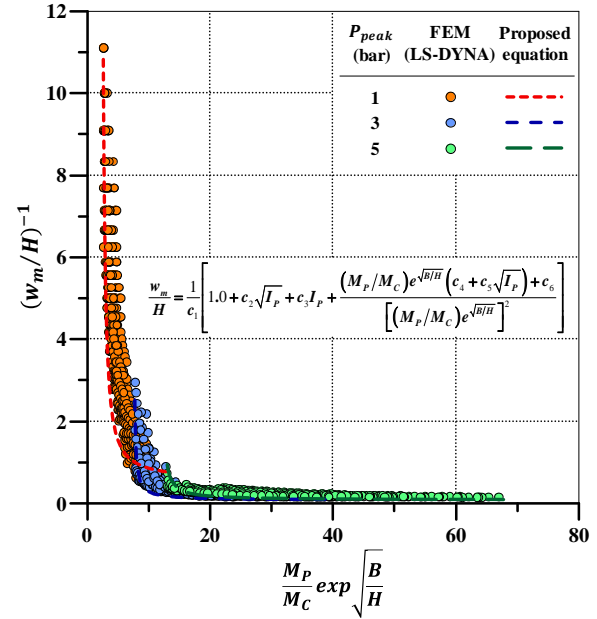
$$\frac{w_m}{H} = \frac{1}{c_1} \left[\frac{1.0 + c_2 \sqrt{I_P} + c_3 I_P}{(M_P/M_C) e^{\sqrt{B/H}} (c_4 + c_5 \sqrt{I_P}) + c_6} + \frac{(M_P/M_C) e^{\sqrt{B/H}}}{[(M_P/M_C) e^{\sqrt{B/H}}]^2} \right] \quad (5)$$

where $c_1 = -0.025$, $c_2 = -19.66$, $c_3 = 68.7$, $c_4 = 3.512$, $c_5 = 52.4$ and $c_6 = 0.2$ are the coefficients.

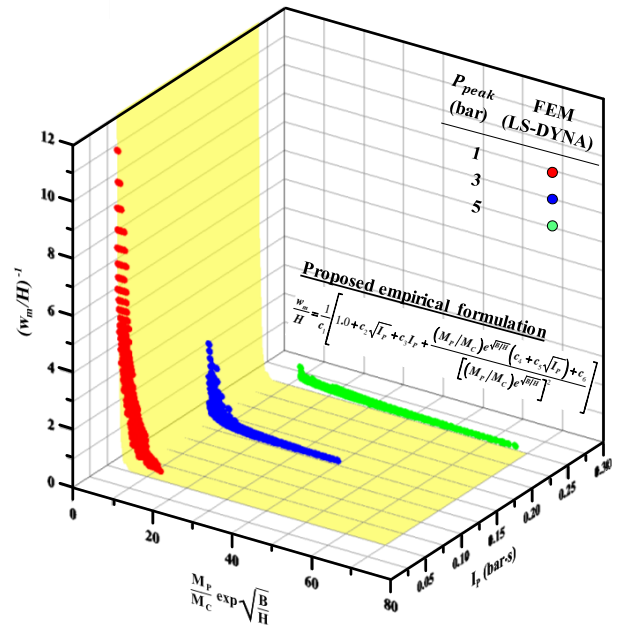
4. Discussion

Design blast load is a function of explosive source location, as well as many other factors including, but not limited to environmental characteristics (e.g., wind speed and direction), quantity and speed of gas leakage, among others. One reliable method of determining the design blast load is by conducting CFD analyses, as explained by (Lei *et al.* 2015). However, it is the intent of the authors to restrict the design parameters to include only geometry, material, and load condition, which can be easily obtained by any user of the proposed empirical equation.

The proposed empirical equation with a coefficient of determination ($R^2 = 0.9212$) can be used to predict maximum structural response of corrugated blast walls due to explosion loadings within a short time. As shown in Fig. 10(b), the proposed empirical formulation does not fit perfectly with obtained FE simulations results. The 3D surface equation, however, may not allow the underestimation of the maximum deflection of the blast



(a) 2-dimensional plot



(b) 3-dimensional plot

Fig. 10 Proposed empirical formulation by 2D and 3D plot (Detailed coefficients can be referred to Eq. (5))

wall.

It can be used before further detailed analysis. In addition, some discrepancies may occur if the connecting parts are considered, as shown in Fig. 2. Furthermore, the proposed equation does not give detailed insights on the time history of failure progression. Thus, nonlinear finite element analyses (NLFEA) may be needed in order to make further justifications on the design. It can, however, be used during the initial design stage of the blast wall, such as the pre-FEED (Front-End-Engineering-Design).

In the elastic range, no permanent deformation was allowed. The maximum elastic moment, M_c occurs at the onset of yielding at the outermost fibers of the flanges.

Further increase in the applied blast pressure leads to the development of plastic moment in the plastic zones. It is associated with the decrease of the elastic core, which exists along the neutral axis at the midsection of the web. Full plastic deformation is attained when the remaining elastic core approaches zero, during which the strength of the structure becomes exhausted, followed by a total collapse.

Contrary to general design practice, higher design peak pressures, i.e., 3 and 5 bars were considered in present study to estimate the nonlinear responses of blast walls subjected to extreme load conditions. The outcome of these “rough” estimations may be taken as a preliminary attempt to be used as reference to more in-depth future studies.

Although buckling behaviors have been detected in some of the models, it was not directly addressed in this study. Logically, it was observed that as the angle of corrugation increases, the shear effect also increases. Thus, the tendency of panel buckling becomes more dominant at the possible failure mode. The methodology for assessing the local buckling responses at webs and flanges of corrugated sections can be referred to the TN5 (Brewerton 1999).

In the present study, an empirical formulation in the shape of a 3D surface curve is proposed to predict maximum deformation of blast wall. It is verified that this proposed empirical formulation shows good agreement with the LS-DYNA simulation results ($R^2 = 0.92$). The benefits of including the connection behaviour in the design of the blast wall system were demonstrated in this study, which is in line with the suggestions highlighted in HSE-RR-404 (Schleyer and Langdon 2006). It is recommended that the effect of connecting parts on maximum deflection of blast wall should be further investigated.

5. Conclusions

It is well recognised that space optimisation of the topside area of offshore oil and gas production facilities is a significant requirement. There is numerous production equipment installed on the topside, together with the cabin area and pedestrian road. In order to protect workers from fire and explosion, installing offshore blast walls is compulsory. A study on the optimisation of the topside space is getting more essential, especially the prediction of the maximum deflection of the blast wall. It is needed to design the walkway between the facilities and the cabin area.

Therefore, the present study proposes an empirical formulation to predict the maximum deflection of the blast wall, for this may be useful to optimise the space of the topside area. The outcome-empirical formulation-shows good agreement ($R^2 = 0.9212$) with the LS-DYNA numerical simulation results using the finite element method (FEM). It is expected that additional design parameters and considerations, for instance, different materials, geometrical configurations, and boundary conditions, i.e. fixed end conditions, be covered and advanced empirical formulation be developed by future studies.

Acknowledgements

This study was undertaken at Ocean and Ship Technology (OST) at Universiti Teknologi PETRONAS. This research was supported by the Technology Innovation Program (Grant No.: 10053121 and 10051279) funded by the Ministry of Trade, Industry & Energy (MI, Korea). The authors would also like to thank for the great support of POSTECH, POSCO, Republic of Korea. This study is also part of Mr. W.C.K. Ng's MSc. dissertation in Universiti Teknologi PETRONAS, Malaysia.

References

- Biggs, J.M. (1964), *Introduction to Structural Dynamics*, McGraw-Hill Companies, New York, U.S.A.
- Boh, J., Choo, Y. and Louca L. (2004), “Design and numerical assessment of blast walls subjected to hydrocarbon explosions”, *Proceedings of the the 14th International Offshore and Polar Engineering Conference (ISOPE 2004)*, Toulon, France, May.
- Brewerton, R. (1999), *Technical Note 5: Design Guide for Stainless Steel Blast Walls*, Fire and Blast Information Group (FABIG), Berkshire, U.K.
- Caldwell, J.B. (1955), “The strength of corrugated plating for ships bulkheads”, *Tran RINA*, **97**, 495-522.
- Caldwell, J.B. (1965), “Ultimate longitudinal strength”, *Tran RINA*, **107**, 411-430.
- Cormie, D., Mays, G. and Smith, P. (2009), *Blast Effects on Buildings*, 2nd Edition, ICE Publishing, London, U.K.
- Cui, W. and Mansour, A.E. (1998), “Effects of welding distortions and residual stresses on the ultimate strength of long rectangular plates under uniaxial compression”, *Mar. Struct.*, **11**(6), 251-269.
- DNV (2010), *Recommended Practice (RP-C204)*, Design Against Accidental Loads, Det Norske Veritas, Oslo, Norway.
- Kim, D.K. and Lim, H.L. (2018), “Ultimate strength assessment of a stiffened panel by developing a refined empirical formulation”, *Eng. Struct.*, Under Revision.
- Kim, D.K., Incecik, A., Choi, H.S., Wong, E.W.C., Yu, S.Y. and Park, K.S. (2018a), “A simplified method to predict fatigue damage of offshore riser subjected to vortex-induced vibration by adopting current index concept”, *Ocean Eng.*, **157**, 401-411.
- Kim, D.K., Kim, B.J., Seo, J.K., Kim, H.B., Zhang, X.M. and Paik, J.K. (2014), “Time-dependent residual ultimate longitudinal strength-grounding damage index (RD) diagram”, *Ocean Eng.*, **76**, 163-171.
- Kim, D.K., Lim, H.L., Kim, M.S., Hwang, O.J. and Park, K.S. (2017), “An empirical formulation for predicting the ultimate strength of stiffened panels subjected to longitudinal compression”, *Ocean Eng.*, **140**, 270-280.
- Kim, D.K., Ng, W.C.K., Hwang, O.J., Sohn, J.M. and Lee, E.B. (2018b), “Recommended finite element formulations for the analysis of offshore blast walls in an explosion”, *Lat. Am. J. Sol. Struct.*, **15**(10), 1-32.
- Kim, D.K., Poh, B.Y., Lee, J.R. and Paik, J.K. (2018c), “Ultimate strength of initially deflected plate under longitudinal compression: Part I=An advanced empirical formulation”, *Struct. Eng. Mech.*, Accepted.
- Kim, D.K., Wong, E.W.C., Lee, E.B., Yu, S.Y. and Kim, Y.T. (2018d), “A method for the empirical formulation of current profile”, *Ships and Offshore Structures*, In Press, <<https://doi.org/10.1080/17445302.2018.1488340>>.
- Koh, B.C. and Kikuchi, N. (1987), “New improved hourglass control for bilinear and trilinear elements in anisotropic linear

- elasticity”, *Comp. Meth. Appl. Mech. Eng.*, **65**(1), 1-46.
- Lei, H.Y., Lee, J.C., Li, C.B., Ha, Y.C., Seo, J.K., Kim, B.J. and Paik, J.K. (2015), “Cost-benefit analysis of corrugated blast walls”, *Ships Offshore Struct.*, **10**(5), 565-574.
- Liang, Y.H., Louca, L.A. and Hobbs, R.E. (2006), “A simplified method in the static plastic analysis of corrugated steel panels”, *J. Strain Analy. Eng. Des.*, **41**(2), 135-149.
- Liao, J.J. and Ma, G. (2018), “Energy absorption of the ring stiffened tubes and the application in blast wall design”, *Struct. Eng. Mech.*, **66**(6), 713-727.
- Lin, Y.T. (1985), “Structural longitudinal ship modelling”, Ph.D. Dissertation, University of Glasgow, Scotland, U.K.
- Louca, L.A. and Fallah, A.S. (2010), *Chapter 10-The Use of Composites in Blast-Resistant Walls*, In N. Uddin (Ed.), *Blast Protection of Civil Infrastructures and Vehicles Using Composites*, Woodhead Publishing, Cambridge, U.K.
- Louca, L.A., Boh, J.W. and Choo, Y.S. (2004), “Design and analysis of stainless steel profiled blast barriers”, *J. Constr. Steel Res.*, **60**(12), 1699-1723.
- Macneal, R.H. and Harder, R.L. (1985), “A proposed standard set of problems to test finite element accuracy”, *Fin. Elem. Analy. Des.*, **1**(1), 3-20.
- Mohd Hairil, M., Kim, D.K., Kim, D.W. and Paik, J.K. (2014), “A time-variant corrosion wastage model for subsea gas pipelines”, *Ships Offshore Struct.*, **9**(2), 161-176.
- OILPRICE (2018), *U.S. Shale Oil Production Rises at Record-Breaking Rate*, <<https://oilprice.com/Energy/Crude-Oil/US-Shale-Oil-Production-Rises-At-Record-Breaking-Rate.html>>.
- Paik, J.K. and Kim, D.K. (2012), “Advanced method for the development of an empirical model to predict time-dependent corrosion wastage”, *Corros. Sci.*, **63**, 51-58.
- Paik, J.K. and Mansour, A.E. (1995), “A simple formulation for predicting the ultimate strength of ships”, *J. Mar. Sci. Technol.*, **1**(1), 52-62.
- Paik, J.K. and Thayamballi, A.K. (1997), “An empirical formulation for predicting the ultimate compressive strength of stiffened panels”, *Proceedings of the 7th International Offshore and Polar Engineering Conference (ISOPE 1997)*, Honolulu, U.S.A., May.
- Paik, J.K., Kim, D.K., Park, D.H., Kim, H.B. and Kim, M.S. (2012), “A new method for assessing the safety of ships damaged by grounding”, *Int. J. Maritime Eng.*, **154**(A1), 1-20.
- Paik, J.K., Kim, D.K., Park, D.H., Kim, H.B., Mansour, A.E. and Caldwell, J.B. (2013), “Modified Paik-Mansour formula for ultimate strength calculations of ship hulls”, *Ships Offshore Struct.*, **8**(3-4), 245-260.
- Paik, J.K., Thayamballi, A.K. and Chun, M.S. (1997), “Theoretical and experimental study on the ultimate strength of corrugated bulkheads”, *J. Ship Res.*, **41**(4), 301-317.
- Paik, J.K., Thayamballi, A.K. and Lee, J.M. (2004), “Effect of initial deflection shape on the ultimate strength behavior of welded steel plates under biaxial compressive loads”, *J. Ship Res.*, **48**(1), 45-60.
- Pan, Y. and Louca, L.A. (1999), “Experimental and numerical studies on the response of stiffened plates subjected to gas explosions”, *J. Constr. Steel Res.*, **52**(2), 171-193.
- Park, B.W. and Cho, S.R. (2006), “Simple design formulae for predicting the residual damage of unstiffened and stiffened plates under explosion loadings”, *Int. J. Imp. Eng.*, **32**(10), 1721-1736.
- Schleyer, G.K. and Langdon, G.S. (2003), *Research Report 124: Pulse Pressure Testing of 1/4 Scale Blast Wall Panels with Connections: Phase I*, Health and Safety Executive (HSE), London, U.K.
- Schleyer, G.K. and Langdon, G.S. (2006), *Research Report 404: Pulse Pressure Testing of 1/4 Scale Blast Wall Panels with Connections: Phase II*, Health and Safety Executive (HSE), London, U.K.
- Schwer, L.E., Key, S.W., Pucik, T.A. and Bindeman, L.P. (2005), “An assessment of the LS-DYNA hourglass formulations via the 3D patch test”, *Proceedings of the 5th European LS-DYNA Users Conference*, Birmingham, U.K., May.
- Seo, J.H., Kim, D.K., Choi, H.S., Yu, S.Y. and Park, K.S. (2018), “Simplified technique for predicting offshore pipeline expansion”, *J. Mar. Sci. Appl.*, **17**(1), 68-78.
- Smith, C.S., Davidson, P.C., Chapman, J.C. and Dowling, P.J. (1988), “Strength and stiffness of ship’s plating under in-plane compression and tension”, *Tran RINA*, **130**, 277-296.
- Sohn, J.M., Kim, S.J., Seo, J.K., Kim, B.J. and Paik, J.K. (2016), “Strength assessment of stiffened blast walls in offshore installations under explosions”, *Ships Offshore Struct.*, **11**(5), 551-560.
- Sohn, J.M., Kim, S.J., Seong, D.J., Kim, B.J., Ha, Y.C., Seo, J.K. and Paik, J.K. (2014), “Structural impact response characteristics of an explosion resistant profiled blast walls in arctic conditions”, *Struct. Eng. Mech.*, **51**(5), 755-771.
- STEO (2018), *Independent Statistics & Analysis by U.S. Energy Information Administration*, Short-Term Energy Outlook, Washington, U.S.A., <https://safety4sea.com/wp-content/uploads/2018/05/EIA-Short-Term-Energy-Outlook-2018_05.pdf>.
- Sun, E.Q. (2006), “Shear locking and hourglassing in MSC Nastran, ABAQUS, and ANSYS”, *Proceedings of the MSC Software Corporation’s 2006 Americas Virtual Product Development Conference*, Detroit, Michigan, U.S.A.
- Ueda, Y., Yao, T., Nakacho, K. and Yuan, M.G. (1992), *Prediction of Welding Residual Stress, Deformation and Ultimate Strength of Plate Panels*, Engineering Design in Welded Constructions, Pergamon Press, Oxford, U.K.
- Zhang, S.M. and Khan, I. (2009), “Buckling and ultimate capability of plates and stiffened panels in axial compression”, *Mar. Struct.*, **22**(4), 791-808.

CC

Appendix

Table A.1(a) Assumed FE types for modelling of target blast wall (Kim *et al.* 2018b)

Model part	FE type				
	Case 1	Case 2	Case 3	Case 4	Case 5
Supporting members	Shell (SH)	Solid (S)	Solid (S)	T-shell (SHT)	T-shell (SHT)
Corrugated panel	Shell (SH)	Shell (SH)	Solid (S)	Shell (SH)	T-shell (SHT)

Note: S, SH, and SHT denote solid, thin-shell, and thick-shell, respectively in present study

Table A.1(b) Selected combinations for the assessment of performance of shell and solid FE formulations (Kim *et al.* 2018b)

FE formulation	Reduced integration (RI)	Full integration (FI)	Hourglass control
Type I SM (Solid) CP (Shell)	√ √	- -	
Type II SM (Solid) CP (Shell)	√ -	- √	IHQ = 5 IHQ = 8
Type III SM (Solid) CP (Shell)	- √	√ -	
Type IV SM (Solid) CP (Shell)	- -	√ √	- -

Note: SM=supporting members modelled by solid elements, CP=corrugated panel modelled by shell elements, IHQ=hourglass control function in LS-DYNA